
Debiasing Concept Bottleneck Models with Instrumental Variables

Mohammad Taha Bahadori David E. Heckerman

Amazon

{bahadorm, heckerma}@amazon.com

Abstract

Concept-based explanation approach is a popular model interpretability tool because it expresses the reasons for a model’s predictions in terms of concepts that are meaningful for the domain experts. In this work, we study the problem of the concepts being correlated with confounding information in the features. We propose a new causal prior graph for modeling the impacts of unobserved variables and a method to remove the impact of confounding information using the instrumental variable techniques. We also model the completeness of the concepts set. Our synthetic and real-world experiments demonstrate the success of our method in removing biases due to confounding and noise from the concepts.

1 Introduction

Explaining the predictions of neural networks through higher level concepts [10, 4, 1, 8] enables model interpretation on data with complex manifold structure such as images. It also allows the use of domain knowledge during the explanation process. The concept-based explanation has been used for medical imaging [2], breast cancer histopathology [7], cardiac MRIs [3], and meteorology [15].

When the set of concepts is carefully selected, we can estimate a model in which the discriminative information flow from the feature vectors \mathbf{x} through the concept vectors \mathbf{c} and reach the labels \mathbf{y} . To this end, we train two models for prediction of the concept vectors from the features denoted by $\hat{\mathbf{c}}(\mathbf{x})$ and the labels from the predicted concept vector $\hat{\mathbf{y}}(\hat{\mathbf{c}})$. This estimation process ensures that for each prediction we have the reasons for the prediction stated in terms of the predicted concept vector $\hat{\mathbf{c}}(\mathbf{x})$.

However, in reality, noise and confounding information (due to e.g. non-discriminative context) can influence both of the feature and concept vectors, resulting in confounded correlations between them. Figure 1 provides an evidence for noise and confounding in the CUB-200-2011 dataset [17]. We train two predictors for the concepts vectors based on features $\hat{\mathbf{c}}(\mathbf{x})$ and labels $\hat{\mathbf{c}}(\mathbf{y})$ and we compare the Spearman correlation coefficients between their predictions and the true ordinal value of the concepts. Having concepts for which $\hat{\mathbf{c}}(\mathbf{x})$ is more accurate than $\hat{\mathbf{c}}(\mathbf{y})$ could be due to noise, or due to hidden variables independent of the labels that spuriously correlated \mathbf{c} and \mathbf{x} , leading to undesirable explanations that include confounding or noise.

In this work, using the Concept Bottleneck Models (CBM) [12, 13] we demonstrate a method for removing the confounding and noise (debiasing) the explanation with concept vectors and extend the results to Testing with Concept Activation Vectors (TCAV) [10] technique. We provide a new causal prior graph to account for the confounding information and concept completeness [18]. We describe the identifiability challenges in our causal prior graph and propose a two-stage estimation procedure. Our two-stage estimation technique defines and predicts debiased concepts such that the predictive information of the features maximally flow through them.

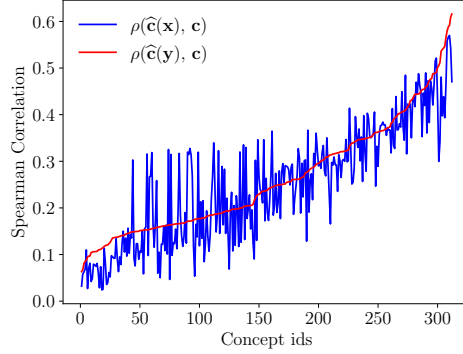


Figure 1: Spearman correlation coefficients (ρ) of the predictors of the concepts given features $\hat{c}(\mathbf{x})$ and labels $\hat{c}(\mathbf{y})$ for the 312 concepts in the test partition of the CUB-200-2011 dataset [17]. 112 concepts can be predicted more accurately with the features rather than the labels. Concept ids in the x-axis are sorted in the increasing $\rho(\hat{c}(\mathbf{y}), \mathbf{c})$ order. We provide the detailed steps to obtain the figure in Section 3.2.

We show that using the labels as instrumental variables, we can successfully remove the impact of the confounding and noise from the predicted concept vectors. The first stage of our proposed procedure has three steps: (1) debias the concept vectors using the labels, (2) predict the debiased concept vectors using the features, and (3) use the predict concept vectors in the second step to predict the labels. In the second stage, we find the residual predictive information in the features that are not in the concepts. We validate the proposed method using a synthetic dataset and the CUB-200-2011 dataset.

2 Methodology

Notations. We follow the notation of [5] and denote random vectors by bold font letters \mathbf{x} and their values by bold symbols \mathbf{x} . The notation $p(\mathbf{x})$ is a probability measure on \mathbf{x} and $dp(\mathbf{x} = \mathbf{x})$ is the infinitesimal probability mass at $\mathbf{x} = \mathbf{x}$. We use $\hat{\mathbf{y}}(\mathbf{x})$ to denote the prediction of \mathbf{y} given \mathbf{x} . In the graphical models, we show the observed and unobserved variables using filled and hollow circles, respectively. To avoid clutter in the equations, without loss of generality, we state the relationships with additive noise.

Problem Statement. We assume that during the training phase, we are given triplets $(\mathbf{x}_i, \mathbf{c}_i, \mathbf{y}_i)$ for $i = 1, \dots, n$ data points. In addition to the regular features \mathbf{x} and labels \mathbf{y} , we are given a human interpretable concepts vector \mathbf{c} for each data point. Each element of the concept vector measures the degree of existence of the corresponding concept in the features. Thus, the concept vector typically have binary or ordinal values. Our goal is to learn to predict \mathbf{y} as a function of \mathbf{x} and use \mathbf{c} for explaining the predictions. Performing in two steps, we first learn a function $\hat{c}(\mathbf{x})$ and then learn another function $\hat{\mathbf{y}}(\hat{c}(\mathbf{x}))$. The prediction $\hat{c}(\mathbf{x})$ is the explanation for our prediction $\hat{\mathbf{y}}$. During the test time, only the features are given and the prediction+explanation algorithm predicts both $\hat{\mathbf{y}}$ and \hat{c} .

2.1 A New Causal Prior Graph for CBMs

Figure 2a shows the ideal situation in explanation via high-level concepts. The generative model corresponding to Figure 2a states that for generating each feature \mathbf{x}_i we first randomly draw the label \mathbf{y}_i . Given the label, we draw the concepts \mathbf{c}_i . Given the concepts, we draw the features. The hierarchy in this graph is from nodes with less detailed information (labels) to more detailed ones (features, images).

This model in Figure 2a is an explanation for the phenomenon in Figure 1, because the noise in generation of the concepts allows the \mathbf{x} — \mathbf{c} edge to be stronger than the \mathbf{c} — \mathbf{y} edge. However, another (non-mutually exclusive) explanation for this phenomenon is the existence of hidden confounders \mathbf{u} shown in Figure 2b. In this graphical model, \mathbf{u} represents the confounders and \mathbf{d} represents the

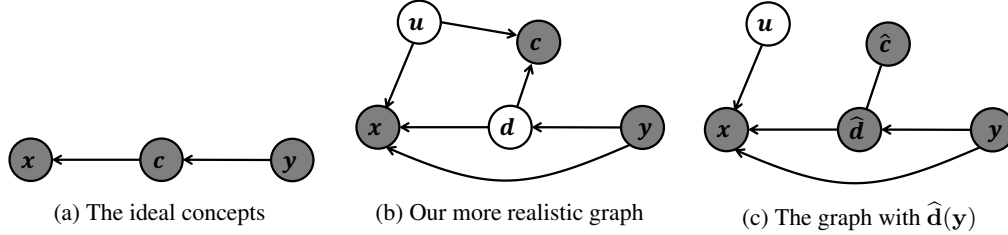


Figure 2: (a) The ideal view of the causal relationships between the features x , concepts c , and labels y . (b) In a more realistic setting, the unobserved confounding variable u impacts both x and c . The discriminative information reaches y through the discriminative part of the concepts d . We also model the completeness of the concepts via a direct edge from the features x to the labels y . (c) When we use $\hat{d}(y) = E[c|y]$ in place of d and c , we eliminate the confounding link $u \rightarrow c$.

unconfounded concepts. Note that we assume that the confounders u and labels y are independent when x and c are not observed.

Another phenomenon captured in Figure 2b is the lack of concept completeness [18]. It describes the situation when the features, compared to the concepts, have additional predictive information about the labels.

The non-linear structural equations corresponding to the causal prior graph in Figure 2b are as follows

$$d = f_1(y) + \varepsilon_d, \quad (1)$$

$$c = d + h(u), \quad (2)$$

$$x = f_2(u, d) + f_3(y) + \varepsilon_x, \quad (3)$$

for some vector functions h , f_1 , f_2 , and f_3 . We have $\varepsilon_d \perp\!\!\!\perp y$ and $u \perp\!\!\!\perp y$. Our definition of d in Eq. (2) does not restrict u , because we simply attribute the difference between c and $f_1(y)$ to a function of the latent confounder u and noise.

Our causal prior graph in Figure 2b corresponds to a generative process in which to generate an observed triplet (x_i, c_i, y_i) we first draw a label y_i and a confounder u_i vector independently. Then we draw the discriminative concepts d_i based on the label and generate the features x_i jointly based on the concepts, label, and the confounder. Finally, we draw the observed concept vector c_i based on the drawn concept and confounder vectors.

Both causal graphs reflect our assumption that the direction of causality is from the labels to concepts and then to the features, $y \rightarrow d \rightarrow x$, to ensure that u and y are marginally independent in Figure 2b. This direction also correspond to moving from more abstract class labels to concepts to detailed features. During estimation, we fit the functions in the $x \rightarrow d \rightarrow y$ direction, because finding the statistical strength of an edge does not depend on its direction.

Estimation of the model in Figure 2b is challenging. Because of the structure of the latent confounders, this model is unidentifiable [14, Chapter 3]. Our solution is to first ignore the $y \rightarrow x$ edge and estimate the $y \rightarrow d \rightarrow x$, then estimate the residuals of the regression using the $y \rightarrow x$ edge. Our two-stage estimation technique ensures that the predictive information of the features maximally flow through the concepts. In the next sections, we focus on the first stage and using the instrumental variables to eliminate the noise and confounding in estimation of the $d \rightarrow x$ link.

2.2 Instrumental Variables

Background on Instrumental Variables. In causal inference, instrumental variables [16, 14] denoted by z are commonly used to find the causal impact of a variable x on y when x and y are jointly influenced by an unobserved confounder u (i.e., $x \leftarrow u \rightarrow y$). The key requirement is that z should be correlated with x but independent of the confounding variable u (i.e. $z \rightarrow x \rightarrow y$ and $z \perp\!\!\!\perp u$). The commonly used 2-stage least squares first regresses x in terms of z to obtain \hat{x} followed by regression of y in terms of \hat{x} . Because of independence between z and u , \hat{x} is also independent of u . Thus, in the second regression the confounding impact of u is eliminated. Our goal is to use the instrumental variable trick again to remove the confounding factors impacting features and concept vectors.

Instrumental Variables for CBMs. In our causal graph in Figure 2b, the label \mathbf{y} is a valid instrument for the study of the relationship between concepts \mathbf{d} and features \mathbf{x} . We predict \mathbf{d} as a function of \mathbf{y} and use it in place of the concepts in the concept bottleneck models. The graphical model corresponding to this procedure is shown in Figure 2c, where the link $\mathbf{u} \rightarrow \mathbf{c}$ is eliminated. In particular, given the independence relationship $\mathbf{y} \perp\!\!\!\perp \mathbf{u}$, we have $\widehat{\mathbf{d}}(\mathbf{y}) = E[\mathbf{c}|\mathbf{y}] \perp\!\!\!\perp \mathbf{h}(\mathbf{u})$. This is the basis for our debiasing method in the next section.

2.3 The Estimation Method.

Our estimation uses the observation that in graph 2b the label vector \mathbf{y} is a valid instrument for removing the correlations due to \mathbf{u} . Combining Eqs. (1) and (2) we have $\mathbf{c} = \mathbf{f}_1(\mathbf{y}) + \mathbf{h}(\mathbf{u}) + \varepsilon_d$. Taking expectation with respect to $p(\mathbf{c}|\mathbf{y})$, we have

$$E[\mathbf{c}|\mathbf{y}] = E[\mathbf{f}_1(\mathbf{y}) + \mathbf{h}(\mathbf{u}) + \varepsilon_d|\mathbf{y}] = \mathbf{f}_1(\mathbf{y}) + E[\mathbf{h}(\mathbf{u})] + E[\varepsilon_d]. \quad (4)$$

The last step is because both \mathbf{u} and ε_d are independent of \mathbf{y} . Thus, two term is constant in terms of \mathbf{x} and \mathbf{y} and can be eliminated after estimation. Eq. (4) allows us to remove the impact of \mathbf{u} and ε_d and estimate the denoised and debiased $\widehat{\mathbf{d}}(\mathbf{y}) = E[\mathbf{c}|\mathbf{y}]$. We find $E[\mathbf{c}|\mathbf{y}]$ using a neural network trained on $(\mathbf{c}_i, \mathbf{y}_i)$ pairs and use them as pseudo-observations in place of \mathbf{d}_i . Given our debiased prediction for the discriminative concepts \mathbf{d}_i , we can perform the CBMs' two-steps of $\mathbf{x} \rightarrow \mathbf{d}$ and $\mathbf{d} \rightarrow \mathbf{y}$ estimation.

Because we use expected values of \mathbf{c} in place of \mathbf{d} during the learning process (i.e., $\widehat{\mathbf{d}}(\mathbf{y}) = E[\mathbf{c}|\mathbf{y}]$), the debiased concept vectors have values within the ranges of original concept vectors \mathbf{c} . Thus, we do not lose the human readability with the debiased concept vectors.

Modeling Uncertainty in Prediction of Concepts. Our empirical observations show that prediction of the concepts from the features can be highly uncertain. Hence, we present a CBM estimator that takes into account the uncertainties in prediction of the concepts. We take the conditional expectation of the labels \mathbf{y} given features \mathbf{x} as follows

$$E[\mathbf{y}|\mathbf{x}] = E[\mathbf{g}_\theta(\widehat{\mathbf{d}})|\mathbf{x}] = \int \mathbf{g}_\theta(\mathbf{d})dp_\phi(\mathbf{d} = \mathbf{d}|\mathbf{x}), \quad (5)$$

where $p_\phi(\mathbf{d}|\mathbf{x})$ is the probability function, parameterized by ϕ , that captures the uncertainty in prediction of labels from features. The $\mathbf{g}_\theta(\cdot)$ function predicts labels from the debiased concepts.

In summary, we perform the following steps to estimate Eq. (5):

1. Train a neural network $\widehat{\mathbf{d}}(\mathbf{y}) = E[\mathbf{c}|\mathbf{y} = \mathbf{y}]$ using $(\mathbf{c}_i, \mathbf{y}_i)$ pairs.
2. Train a neural network as an estimator for $p_{\widehat{\phi}}(\mathbf{d}|\mathbf{x})$ using $(\mathbf{x}_i, \widehat{\mathbf{d}}_i)$ pairs .
3. Use pairs $(\mathbf{x}_i, \mathbf{y}_i)$ to estimate function \mathbf{g}_θ by fitting $\int \mathbf{g}_\theta(\mathbf{d})dp_{\widehat{\phi}}(\mathbf{d} = \mathbf{d}|\mathbf{x})$ to $E[\mathbf{y}|\mathbf{x}]$.
4. [Optional] Fit a neural network $\mathbf{q}(\mathbf{x})$ to the residuals of step 3. The function $\mathbf{q}(\cdot)$ captures the residual information in \mathbf{x} . Compare the improvement in prediction accuracy over the accuracy in step 3 to quantify the degree of concept incompleteness.

Steps 1–3 describe the first stage of estimating the $\mathbf{y} \rightarrow \mathbf{d} \rightarrow \mathbf{x}$ and step 4 describe the second stage of estimating the residual link $\mathbf{y} \rightarrow \mathbf{x}$. In step 3, we approximate the integral using Monte Carlo approach by drawing from the distribution $p_{\widehat{\phi}}(\mathbf{d}|\mathbf{x})$ estimated in step 2. Because we first predict the labels \mathbf{y} using the concepts and then fit the $\mathbf{q}(\mathbf{x})$ to the residuals, we ensure that the predictive information maximally go through the debiased concepts. The last step is optional, because our goal is to compare the predictive power of the features going through the concepts (step 3) with the unrestricted features (step 4). We can omit step 4 and learn an unrestricted predictive model $E[\mathbf{y}|\mathbf{x}]$ and use it for comparison.

A Special Case and Application to TCAV. Choosing a simple multivariate Gaussian distribution $p(\mathbf{d}|\mathbf{x}) = \mathcal{N}(\mathbf{x}, \sigma \mathbf{I})$, $\sigma > 0$, we can show that the above steps are simplified as follows:

1. Learn $\widehat{\mathbf{d}}(\mathbf{y})$ by predicting $\mathbf{y}_i \rightarrow \mathbf{c}_i$.

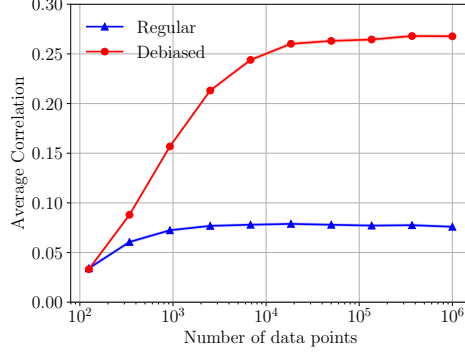


Figure 3: Correlation between the estimated concept vectors and the true discriminative concept vectors as the number of data points grow.

2. Learn $\hat{\mathbf{d}}(\mathbf{x})$ by predicting $\mathbf{x}_i \rightarrow \hat{\mathbf{d}}_i$.
3. Learn $\hat{\mathbf{y}}(\hat{\mathbf{d}})$ by predicting $\hat{\mathbf{d}}_i \rightarrow \mathbf{y}_i$.
4. [Optional] Learn $\mathbf{q}(\mathbf{x})$ to predict the residues $\mathbf{y}_i - \hat{\mathbf{y}}(\hat{\mathbf{d}}_i)$.

The above special case suggests us a simple method for debiasing the results of TCAV [10] analysis. The TCAV method is attractive, because unlike CBMs, it analyzes the existing neural networks and does not need to define a new model. We can use the first step to remove the bias due to the confounding and perform TCAV among \mathbf{d} vectors, instead of \mathbf{c} vectors.

Prior Work on Causal Concept-Based Explanation. Among the existing works on causal concept-based explanation, [6] proposes a different causal prior graph to model the spurious correlations among the concepts and remove them using conditional variational auto-encoders. In contrast, we aim at handling noise and spurious correlations between the features and concepts using the labels as instruments. Which work is more appropriate for a problem depending on the assumptions underlying that problem.

3 Experiments

3.1 Synthetic Data Experiments

We create a synthetic dataset according to the following steps:

1. Generate n vectors $\mathbf{y}_i \in \mathbb{R}^{100}$ with elements distributed according to unit normal distribution $\mathcal{N}(0, 1)$.
2. Generate n vectors $\mathbf{u}_i \in \mathbb{R}^{100}$ with elements distributed according to unit normal distribution $\mathcal{N}(0, 1)$.
3. Generate n vectors $\boldsymbol{\varepsilon}_{c,i} \in \mathbb{R}^{100}$ with elements distributed according to scaled normal distribution $\mathcal{N}(0, \sigma = 0.02)$.
4. Generate n vectors $\boldsymbol{\varepsilon}_{x,i} \in \mathbb{R}^{100}$ with elements distributed according to scaled normal distribution $\mathcal{N}(0, \sigma = 0.02)$.
5. Generate matrices $\mathbf{W}_1, \mathbf{W}_2, \mathbf{W}_3, \mathbf{W}_4 \in \mathbb{R}^{100 \times 100}$ with elements distributed according to scaled normal distribution $\mathcal{N}(0, \sigma = 0.1)$.
6. Compute $\mathbf{d}_i = \mathbf{W}_1 \mathbf{y}_i + \boldsymbol{\varepsilon}_{d,i}$ for $i = 1, \dots, n$.
7. Compute $\mathbf{c}_i = \mathbf{d}_i + \mathbf{W}_2 \mathbf{u}_i$ for $i = 1, \dots, n$.
8. Compute $\mathbf{x}_i = \mathbf{W}_3 \mathbf{d}_i + \mathbf{W}_4 \mathbf{u}_i + \boldsymbol{\varepsilon}_{x,i}$ for $i = 1, \dots, n$.

In Figure 3, we plot the correlation between the true unconfounded and noiseless concepts $\mathbf{W}\mathbf{y}$ and the estimated concept vectors with the regular two-step procedure (without debiasing) and our



Figure 4: Twelve example images where the debiasing using instrumental variables helps. A common pattern is that, the image context has either prevented or misled the annotator from accurate annotation of the concepts. From the left to right, the birds are ‘Brandt Cormorant’, ‘Pelagic Cormorant’, ‘Fish Crow’, ‘Fish Crow’, ‘Fish Crow’, ‘Ivory Gull’, ‘Ivory Gull’, ‘Green Violetear’, ‘Green Violetear’, ‘Cape Glossy Starling’, ‘Northern Waterthrush’, ‘Northern Waterthrush’.

Table 1: Mapping the concept annotations to real values.

Annotation	Certainty	Ordinal Score	Numeric Map
Doesn’t Exist	definitely	0	0
Doesn’t Exist	probably	1	1/6
Doesn’t Exist	guessing	2	2/6
Doesn’t Exist	not visible	3	3/6
Exists	not visible	3	3/6
Exists	guessing	4	4/6
Exists	probably	5	5/6
Exists	definitely	6	1

debiasing method, as a function of sample size n . The results show that the bias due to confounding does not vanish as we increase the sample size and our debiasing technique can make the results closer to the true discriminative concepts.

3.2 CUB Data Experiments

Dataset and preprocessing. We evaluate the performance of the proposed approach on the CUB-200-2011 dataset [17]. The dataset includes 11788 pictures (in 5994/5794 train/test partitions) of 200 different types of birds, annotated both for the bird type and 312 different concepts about each picture. The concept annotations are binary, whether the concept exists or not. However, for each statement, a four-level certainty score has been also assigned: 1: not visible, 2: guessing, 3: probably, and 4: definitely. We combine the binary annotation and the certainty score to create a 7-level ordinal variable as the annotation for each image as summarized in Table 1. For simplicity, we map the 7-level ordinal values to uniformly spaced values in the $[0, 1]$ interval. We randomly choose 15% of the training set and hold out as the validation set.

The result in Figure 1. To compare the association strength between \mathbf{y} and \mathbf{c} with the association strength between \mathbf{x} and \mathbf{c} we train two predictors of concepts $\hat{\mathbf{c}}(\mathbf{x})$ and $\hat{\mathbf{c}}(\mathbf{y})$. We use PyTorch’s pre-trained ResNet152 network [9] for prediction of the concepts from the images. Because the annotations are ordinal numbers, we use the Spearman correlation to find the association strengths. Because \mathbf{y} is a categorical variable, $\hat{\mathbf{c}}(\mathbf{y})$ is simply the average concept annotation scores per each class. The concept ids in the x-axis are sorted in terms of increasing values of $\rho(\hat{\mathbf{c}}(\mathbf{y}), \mathbf{c})$.

The top ten concepts with the largest values of $\rho(\hat{\mathbf{c}}(\mathbf{x}), \mathbf{c}) - \rho(\hat{\mathbf{c}}(\mathbf{y}), \mathbf{c})$ are ‘has back color::green’, ‘has upper tail color::green’, ‘has upper tail color::orange’, ‘has upper tail color::pink’, ‘has back color::rufous’, ‘has upper tail color::purple’, ‘has back color::pink’, ‘has upper tail color::iridescent’, ‘has back color::purple’, ‘has back color::iridescent’. These concepts are all related to color and can be easily confounded by the context of the images.

Training details for Eq. (5). We model the distribution of concept logits as independent Gaussians with their means equal to the ResNet152 logit outputs. We estimate the variance for each dimension by using the logits of the true annotation scores that are clamped into $[0.05, 0.95]$ to avoid large logit numbers. In each iteration of the training algorithm, we draw 25 samples from the $p(\mathbf{d}|\mathbf{x})$. Predictor of labels from concepts (the function $g(\cdot)$ in Eq. (5)) is a three-layer feed-forward neural network with hidden layer sizes (312, 312, 200). There is a skip connection from the input to the

penultimate layer. We model the residual function $q(\cdot)$ with another pretrained ResNet152 function. All algorithms are trained with Adam optimization algorithm [11].

Quantitative experiments. Comparing to the baseline algorithm, our debiasing technique increases the average Spearman correlation between $\hat{c}(x)$ and $\hat{c}(y)$ from 0.406 to 0.508. For the above 10 concepts, our algorithm increases the average Spearman correlation from 0.283 to 0.389. Our debiasing algorithm also improves the generalization in prediction of the image labels. It improves the top-5 accuracy of predicting the images from 39.5% to 49.3%.

Analysis of the results. In Figure 4, we show 12 images for which the $\hat{c}(y)$ and c are significantly different. A common pattern among the examples is that the context of the image does not allow accurate annotations by the annotators. In images 3, 4, 5, 6, 7, 11, and 12 in Figure 4 the ten color-related concepts listed above are all set to 0.5, indicating that the annotators have failed in annotation. However, our algorithm correctly identifies that for example Ivory Gulls do not have green-colored backs by predicting $\hat{c} = 0.08$ which is closer to $\hat{c}(y) = 0.06$ than the true $c = 0.5$.

Another pattern is the impact of the color of the environment on the accuracy of the annotations. For example, the second image from the left is an image of Pelagic cormorant, whose back and upper tail colors are unlikely to be green with per-class average of 0.12 and 0.07, respectively. However, because of the color of the image and the reflections, the annotator has assigned 1.0 to both of ‘has back color::green’ and ‘has upper tail color::green’ concepts. Our algorithm predicts 0.11 and 0.16 for these two features respectively, which are closer to the per-class average.

4 Conclusions and Future Works

Studying the concept-based explanation techniques, we provided evidences for potential existence of an unobserved latent variable, independent of the labels, that creates associations between the features and concepts. We proposed a new causal prior graph that models the impact of the noise and latent confounding from the estimated concepts. We showed that using the labels as instruments, we can remove the impact of the context from the explanations. Our experiments showed that our debiasing technique not only improves the quality of the explanations, but also improve the accuracy of predicting labels through the concepts. As future work, we will investigate other instrumental variable techniques to find the most accurate debiasing method.

References

- [1] Lennart Brocki and Neo Christopher Chung. Concept saliency maps to visualize relevant features in deep generative models. *arXiv:1910.13140*, 2019.
- [2] Carrie J Cai, Emily Reif, Narayan Hegde, Jason Hipp, Been Kim, Daniel Smilkov, Martin Wattenberg, Fernanda Viegas, Greg S Corrado, Martin C Stumpe, et al. Human-centered tools for coping with imperfect algorithms during medical decision-making. In *CHI*, 2019.
- [3] James R Clough, Ilkay Oksuz, Esther Puyol-Antón, Bram Ruijsink, Andrew P King, and Julia A Schnabel. Global and local interpretability for cardiac mri classification. In *MICCAI*, 2019.
- [4] Amirata Ghorbani, James Wexler, James Y Zou, and Been Kim. Towards automatic concept-based explanations. In *NeurIPS*, pages 9273–9282, 2019.
- [5] Ian Goodfellow, Yoshua Bengio, and Aaron Courville. *Deep learning*. MIT press, 2016.
- [6] Yash Goyal, Uri Shalit, and Been Kim. Explaining classifiers with causal concept effect (cace). *arXiv:1907.07165*, 2019.
- [7] Mara Graziani, Vincent Andrearczyk, and Henning Müller. Regression concept vectors for bidirectional explanations in histopathology. In *Understanding and Interpreting Machine Learning in Medical Image Computing Applications*, pages 124–132. Springer, 2018.
- [8] Mandana Hamidi-Haines, Zhongang Qi, Alan Fern, Fuxin Li, and Prasad Tadepalli. Interactive naming for explaining deep neural networks: A formative study. *arXiv:1812.07150*, 2018.
- [9] Kaiming He, Xiangyu Zhang, Shaoqing Ren, and Jian Sun. Deep residual learning for image recognition. In *CVPR*, 2016.

- [10] Been Kim, Martin Wattenberg, Justin Gilmer, Carrie Cai, James Wexler, Fernanda Viegas, et al. Interpretability beyond feature attribution: Quantitative testing with concept activation vectors (tcav). In *ICML*, pages 2668–2677, 2018.
- [11] Diederik P Kingma and Jimmy Ba. Adam: A method for stochastic optimization. *arXiv preprint arXiv:1412.6980*, 2014.
- [12] Pang Wei Koh, Thao Nguyen, Yew Siang Tang, Stephen Mussmann, Emma Pierson, Been Kim, and Percy Liang. Concept Bottleneck Models. In *ICML*, 2020.
- [13] Max Losch, Mario Fritz, and Bernt Schiele. Interpretability beyond classification output: Semantic bottleneck networks. *arXiv:1907.10882*, 2019.
- [14] Judea Pearl. *Causality*. Cambridge university press, 2009.
- [15] Conner Sprague, Eric B Wendoloski, and Ingrid Guch. Interpretable ai for deep learning- based meteorological applications. In *American Meteorological Society Annual Meeting*. AMS, 2019.
- [16] James H Stock. Instrumental variables in statistics and econometrics. *International Encyclopedia of the Social & Behavioral Sciences*, 2015.
- [17] C. Wah, S. Branson, P. Welinder, P. Perona, and S. Belongie. The Caltech-UCSD Birds-200-2011 Dataset. Technical Report CNS-TR-2011-001, California Institute of Technology, 2011.
- [18] Chih-Kuan Yeh, Been Kim, Sercan O Arik, Chun-Liang Li, Pradeep Ravikumar, and Tomas Pfister. On concept-based explanations in deep neural networks. *arXiv:1910.07969*, 2019.